Ab initio augmented space recursion to study complex multicomponent materials: Application to the pseudobinary alloy $Ni_{1-x}Pt_xAl$

Aftab Alam
Department of Materials Science and Engineering, University of Illinois, Urbana-Champaign, Illinois 61801, USA

T. Saha-Dasgupta and Abhijit Mookerjee
Advanced Materials Research Unit, S.N. Bose National Center for Basic Sciences, JD Block, Sector III, Salt Lake City, Kolkata 700 098, India

(Received 19 October 2009; published 1 February 2010)

Using first-principles density-functional calculations, we studied the electronic structure and phase stability of the pseudobinary alloys. The calculations have been carried out using the augmented space recursion based on the all electron, tight-binding linear muffin-tin orbital basis. This work, in particular, provides a further generalization of our earlier developed technique to the case of systems of multiple sublattices with varying degree of disorder on them. We showcase the feasibility of our formalism by applying to a face-centered tetragonal-based pseudobinary $(Ni_{1-x}Pt_x)_3Al$ alloy system. Based on the calculation of effective pair interactions and their lattice Fourier transform, our phase stability search yields two stable superordered structures, namely, $L1_0$-type Ni_2PtAl and $L1_0$-type $NiPt_2Al$ of which the latter has been observed experimentally. An estimate of the minima in the effective pair potential surface $V(\mathbf{k})$ predicted the order-disorder transition temperatures of the two stable structures to be ~1027 and ~1379 K, respectively. The results are in agreement with the previous findings, proving the effectiveness of augmented space recursive technique in dealing with systems of multiple sublattices with varying degree of disorder on them. Our calculated additional physical quantities such as short-range order maps can be compared with future experimental studies.

DOI: 10.1103/PhysRevB.81.054201 PACS number(s): 71.15.Mb, 64.60.Cn, 71.20.Be

I. INTRODUCTION

Metals and alloys are materials about which there is continuing scientific and technological interest. The key issues in alloys are the identification of stable phases and the instability of these stable phases on raising temperature as one varies the composition. Valuable knowledge of phase stability in metallic alloys comes from both theory and experiment. Developing theoretical methods lead to microscopic understanding of stability which in turn provides clues for designing materials with desired or improved properties. A major component of such an understanding is the knowledge of the electronic structure of alloys, both in the ordered and the disordered phases.

A vast majority of the work on disordered alloys have been based on the ubiquitous single-site coherent-potential approximation (CPA).[1–7] CPA is indeed a powerful mean-field approximation which maintains the Herglotz analytic properties of the approximated configuration-averaged Green's function. However, it has long been recognized that, being a single-site approximation, it cannot accurately take into account effects of either correlated configuration fluctuations of the neighborhood of a site or intrinsic off-diagonal disorder. Of the plethora of generalizations of the CPA only a few maintain the proper analytic properties and local symmetries of the approximated averaged quantities. Only these have survived the test of time: among them are the special quasirandom structures (SQS),[8] locally self-consistent multiple-scattering method,[9] locally self-consistent Green's function approach,[10] the nonlocal CPA,[11–13] the traveling-cluster approximation (TCA),[14–17] the itinerant coherent-potential approximation (ICPA),[18] and the augmented space recursion (ASR).[19] The last three are based on the augmented space formalism proposed by one of us.[20,21] Over the years, the ASR coupled with the tight-binding linear muffin-tin orbitals (TB-LMTO) method[22] has been utilized to predict varieties of properties of disordered solids. As indicated above, one of the most interesting features of this technique is its capability of taking into account the effects at a site of configuration fluctuations of its near neighborhood, at the same time maintaining analytical properties and symmetries of the configuration-averaged resolvents. Some examples of this are the effects of local lattice distortion arising out of the large size mismatch of the constituent atoms, for example, as in CuBe,[23] short ranged ordering due to local chemistry in a variety of alloys,[24–26] the phonon problem[27] where the disorder in the dynamical matrices is essentially off-diagonal and the dynamical matrix sum-rule couples the disorder in the diagonal and off-diagonal elements, and in optical[28] and thermal transport properties[29] of disordered alloys.

Although this is a powerful technique, its application to phase stability has been restricted so far mostly to cubic alloy systems[30–36] with one atom in the unit cell. There have been a few ASR works on structures with many atoms per unit cell.[37,38] Very recently, ASR has been extended to hexagonal alloy systems[39] with two atoms in the unit cell. Extension of the ASR method to handle crystal structures with multiple sublattices where different sublattices have varying degree of disorder is an important issue. This would enable us to study complex materials with many atoms per unit cell, where the alloying occurs normally in one particular sublattice. This would, for example, enable its usage to perovskite-like materials with a general formula ABO_3 where the sub-

stitution is often made only in the A or B sublattice or both.

As a test case application of our technique we shall study the electronic structure of a class of pseudobinary alloys $(A_{1-x}B_x)_3C$, with two interpenetrating sublattices. One is ordered with only the specie C occupying its sites while the other is disordered with species A and B randomly occupying its sites with probabilities proportional to their concentrations: x and $1-x$. In that sense the disorder in the system is partial. In particular, we will study the pseudobinary limit of the face-centered tetragonal-based ternary alloy system Ni-Pt-Al. The $L1_2$ structured intermetallic compound Ni_3Al, which is the major strengthening phase of Ni-based superalloys, has excellent high-temperature characteristics. The density of Ni_3Al is considerably lower than that of the other Ni-based superalloys. Although the single crystal Ni_3Al is a very good ductile material, the earlier studies show that by ternary alloying of electron donor elements in Ni_3Al, one can further improve its ductility.[40] In addition, it has been found that the addition of Pt to β NiAl as well as $\gamma'+\gamma$ NiAl alloys can significantly enhance their high-temperature oxidation resistance[41] which make them attractive candidates for application in gas-turbine engines. Recent experiments by Gleeson *et al.*,[41] Kamm and Milligan,[42] and Meininger and Ellner[43] predicted the stability of ternary α Ni-Pt-Al phase with $L1_0$-type ordered face-centered tetragonal structure which exists over a large composition range. It has been established both theoretically[44] and experimentally[45] that Pt has a strong tendency to occupy the Ni sites (face centers) in Ni_3Al, which clearly suggests, the existence of pseudobinary $(Ni_{1-x}Pt_x)_3$ Al alloys in which the Al atoms exclusively occupy the cube corners and the Ni and Pt atoms substitutionally occupy the face centers of a $L1_2$ unit cell (see Fig. 1). This alloy system has been studied both theoretically[46] and experimentally[42,43] reporting presence of superordered structures. Existence of both theoretical as well as experimental studies makes this alloy system an ideal candidate as a testing ground for our formalism.

Further reason behind choosing this alloy is the fact that the parent Ni-Pt alloy on its own has always been a difficult system to study because of several reasons,[32] e.g., effects due to large charge transfer and the large size mismatch between the alloy constituents. There exists a series of papers[47–50] in literature on ordered and substitutionally disordered Ni-Pt systems which have shown the importance of the inclusion of relativistic corrections to correctly predict their thermodynamic properties. A theory for the pseudobinary $(Ni_{1-x}Pt_x)_3Al$ alloys, therefore must also take into account all these effects. In an effort to make accurate predictions, we have performed a scalar-relativistic treatment of the Kohn-Sham equation and have taken into account the effects of large charge-transfer and lattice relaxation effects on the electronic structure through augmented space method.

In addition to the electronic structure, we shall also examine the phase stability of such systems. In order to study the phase stability in such pseudobinary-alloy systems, we shall start from a completely disordered phase, set up a perturbation in the form of concentration fluctuations associated with an ordered phase and study whether the alloy can sustain such a perturbation. In terms of methodologies, we shall use the recursion-based orbital peeling (OP) method introduced by Burke[51] for the direct calculation of small energy differences. OP will be carried out in conjunction with the ASR coupled with the tight-binding linear muffin-tin orbitals (TB-LMTO) basis. The analysis will be based on the calculation of quantities such as mixing enthalpies, pair potentials, ordering energies, mean-field transition temperatures, and the short-range-order (SRO) maps.

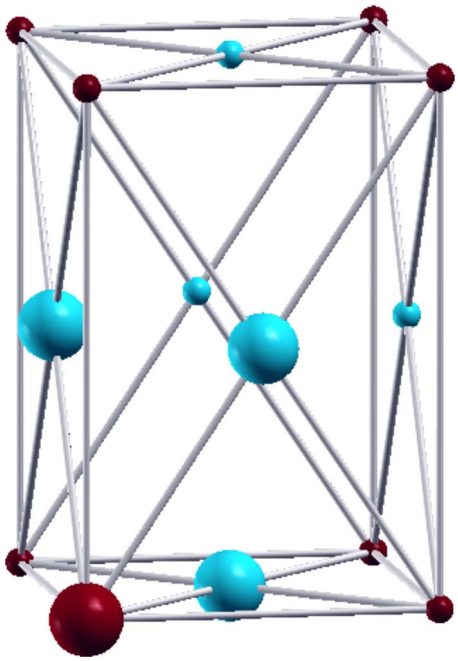

FIG. 1. (Color online) The $L1_2$ unit cell. The atoms in the unit cell are shown as large spheres while those related by lattice translation are shown as small spheres. An A_3B $L1_2$ unit cell consists of two types of lattice sites: those at face centers occupied by A atoms and those at cube corners occupied by B atoms. The two types of lattice sites are shown as (red) dark and (cyan) light spheres, respectively. The pseudobinary $(Ni_{1-x}Pt_x)_3Al$ system basically consists of two distinct sublattices in which cube-corner sites (the sublattice I) are exclusively occupied by Al atoms while the Ni and Pt atoms substitutionally occupy the face-centered sites (sublattice II).

The rest of the paper is organized as follows. In Sec. II, we shall describe in brief our formalism for the electronic structure and phase stability calculations. The results on the density of states (DOS) and the stability of ordered structures for $(Ni_{1-x}Pt_x)_3Al$ alloys will be discussed in Sec. III. Concluding remarks will be given in the final section.

II. FORMALISM

A. TB-LMTO-ASR for complex disordered structures

The TB-LMTO-ASR begins by expressing the "Hamiltonian" of the Kohn-Sham equation in the minimal basis set of screened linear muffin-tin orbitals. In the most localized β representation, the second-order TB-LMTO Hamiltonian[52] for a complex structured compound with multiple sublattices can be expressed as

$$\mathbf{H}^{(2)} = \mathbf{H}^{(1)} - \mathbf{h}\ \mathbf{o}\ \mathbf{h}, \tag{1}$$

where

$$\mathbf{H}^{(1)} = \sum_{R\alpha_s L} C_{RL}^{\alpha_s} \mathbf{P}_{RL}^{\alpha_s} + \boldsymbol{\Delta}^{1/2} \mathbf{S} \boldsymbol{\Delta}^{1/2}$$

and

$$\boldsymbol{\Delta}^{1/2} = \sum_{R\alpha_s L} \Delta_{RL}^{\alpha_s\ 1/2} \mathbf{P}_{RL}^{\alpha_s},$$

$$\mathbf{S} = \sum_{R\alpha_s L} \sum_{R'\alpha_{s'}L'} S_{RL,R'L'}^{\alpha_s\alpha_{s'}} \mathbf{T}_{RL,R'L'}^{\alpha_s\alpha_{s'}},$$

$$\mathbf{h} = \mathbf{H}^{(1)} - \sum_{R\alpha_s L} E_{\nu RL}^{\alpha_s} \mathbf{P}_{RL}^{\alpha_s},$$

$$\mathbf{o} = \sum_{R\alpha_s L} O_{RL}^{\alpha_s} \mathbf{P}_{RL}^{\alpha_s}. \tag{2}$$

Here R and R' denote the position of the unit cells of the lattice: the basis is thus a real space based one. $\mathrm{L}=(\ell m)$ is the composite angular momentum index. α_s denotes the αth atom within the unit cell sitting on the sth sublattice. The actual atomic position is $\mathrm{R}+\xi^{\alpha_s}$, where ξ^{α_s} denotes the position of the αth atom on the sth sublattice.

The quantities X_{RL}^{α}, where $X=C$, $\Delta^{1/2}$, E_ν, and O are the potential parameters which describe the scattering properties of the atomic potentials at $R+\xi^{\alpha}$. For multisublattice multicomponent alloys, the potential parameters can take on values depending on which sublattice it belongs to. S is the structure matrix which characterizes the full multisublattice geometry. $\mathbf{P}$ and $\mathbf{T}$ are the projection and transfer operators in the Hilbert space spanned by the TB-LMTO basis $|R\alpha_s L\rangle$.

Turning to disorder in the system, the most general statement that we may make is that the occupation of the lattice points in each sublattice may be different. In the case we are interested in, as seen in Fig. 1, there are two types of sublattices: the sites belonging to the first sublattice are ordered with Al atoms occupying all of them while the sites belonging to the second sublattice is randomly occupied by either Ni or Pt atoms. In general, even the first sublattice could have been disordered in a different material. For such binary disorder we can introduce random, sublattice and site-dependent occupation variables $n_R^{\alpha_s}$, which take the values 1 and 0 randomly according to whether the site $R+\xi^{\alpha_s}$ is occupied by an A or a B type of atom. The potential parameters $X_{RL}^{\alpha_s}$ can then be expressed as

$$X_{RL}^{\alpha_s} = X_L^A n_R^{\alpha_s} + X_L^B (1 - n_R^{\alpha_s}).$$

For homogeneous disorder on a particular sublattice s, the random occupation variable $n_R^{\alpha_s}$ takes the value 1 with probability $x_A^{\alpha_s}$ and 0 with probability $(1-x_A^{\alpha_s})$.

The augmented space formulation[20,21] now proceeds as follows: taking clue from measurement theory techniques, all the random variables $n_R^{\alpha_s}$ are associated with operators $\mathbf{N}_R^{\alpha_s}$. The results of measurement are the eigenvalues of these operators and their projected spectral densities are the probability densities of the variables $n_R^{\alpha_s}$. The eigenstates of these operators: $\{|\lambda_R^{\alpha_s}\rangle\}$ span the *configuration space* $\phi_R^{\alpha_s}$ of $n_R^{\alpha_s}$. We prefer to work in the basis in which the operators are tridiagonal. For the binary distribution we label this basis by $0_R^{\alpha_s}$ and $1_R^{\alpha_s}$. The full configuration space of all the variables $\{n_R^{\alpha_s}\}$ is $\Phi=\prod^{\otimes}\phi_R^{\alpha_s}$. A particular basis in this space is characterized by its "cardinality sequence" which is the sequence of sites $\{R_n\}$ at which we have a state $1_{R_n}^{n_s}$. Any random local potential parameter $X_{RL}^{\alpha_s}$ in the Hamiltonian is replaced by an operator $\hat{\mathbf{X}}_{RL}^{\alpha_s} \in \Phi$ and may be expressed as

$$\hat{\mathbf{X}}_{RL}^{\alpha_s} = A(X_L)\hat{\mathbf{I}} + B(X_L)\hat{\mathbf{P}}_{1_R^{\alpha_s}} + F(X_L)\hat{\mathbf{T}}_{0_R^{\alpha_s}1_R^{\alpha_s}}, \tag{3}$$

where

$$A(X_L) = x_A^{\alpha_s} X_L^A + (1 - x_A^{\alpha_s}) X_L^B,$$

$$B(X_L) = (2x_A^{\alpha_s} - 1)\,\delta X_L,$$

$$F(X_L) = \sqrt{x_A^{\alpha_s}(1 - x_A^{\alpha_s})}\,\delta X_L,$$

$$\delta X_L = X_L^A - X_L^B,$$

where $\hat{\mathbf{P}}_{1_R^{\alpha_s}}$ are the projection operators in the configuration space which essentially count the number of configuration fluctuations locally at site R. $\hat{\mathbf{T}}_{0_R^{\alpha_s}1_R^{\alpha_s}}$ on the other hand are the transfer operators in the same space which either create or annihilate configuration fluctuations again *locally* at R.

The augmented space theorem[20] tells us that the configuration average of any function of $\{n_R^{\alpha_s}\}$ can be written as a matrix element in "configuration" space of an operator which is the same functional of $\{\mathbf{N}_R^{\alpha_s}\}$,

$$\langle\langle f[\{n_R^{\alpha_s}\}]\rangle\rangle = \langle\{\emptyset\}|\hat{\mathbf{f}}[\{\mathbf{N}_R^{\alpha_s}\}]|\{\emptyset\}\rangle. \tag{4}$$

The state $\{\emptyset\}$ denotes a configuration with $0_R^{n_s}$ at *every* site. The augmented space formalism gives the configuration-averaged Green's function as a matrix element of an augmented resolvent in the space $\mathcal{H}\otimes\Phi$,

$$\langle\langle G(z)\rangle\rangle_{RL,R'L'}^{\alpha_s\alpha_{s'}} = \langle\{\emptyset\}\otimes R\alpha_s L|(z\tilde{\mathbf{I}} - \tilde{\mathbf{H}}^{(2)})^{-1}|\{\emptyset\}\otimes R'\alpha_{s'}L'\rangle, \tag{5}$$

where $\tilde{\mathbf{H}}^{(2)}$ is an operator in the enlarged augmented space $\mathcal{H}\otimes\Phi$,

$$\tilde{\mathbf{H}}^{(2)} = \tilde{\mathbf{H}}^{(1)} - \tilde{\mathbf{h}}\tilde{\mathbf{o}}\tilde{\mathbf{h}}, \tag{6}$$

where

$$\tilde{\mathbf{H}}^{(1)} = \sum_{R\alpha_s L} \hat{\mathbf{C}}_{RL}^{\alpha_s} \otimes \mathbf{P}_{RL}^{\alpha_s} + \tilde{\boldsymbol{\Delta}}^{1/2} \otimes \tilde{\mathbf{S}} \otimes \tilde{\boldsymbol{\Delta}}^{1/2}$$

and

$$\tilde{\boldsymbol{\Delta}}^{1/2} = \sum_{R\alpha_s L} (\hat{\boldsymbol{\Delta}}_{RL}^{\alpha_s})^{1/2} \otimes \mathbf{P}_{RL}^{\alpha_s},$$

$$\tilde{\mathbf{S}} = \sum_{R\alpha_s L} \sum_{R'\alpha_{s'}L'} S_{RL,R'L'}^{\alpha_s\alpha_{s'}} \hat{\mathbf{I}} \otimes \mathbf{T}_{RL,R'L'}^{\alpha_s\alpha_{s'}},$$

$$\tilde{\mathbf{h}} = \tilde{\mathbf{H}}^{(1)} - \sum_{R\alpha_s L} \hat{\mathbf{E}}_{\nu RL}^{\alpha_s} \otimes \mathbf{P}_{RL}^{\alpha_s},$$

$$\tilde{\mathbf{o}} = \sum_{R\alpha_s L} \hat{\mathbf{O}}_{RL}^{\alpha_s} \otimes \mathbf{P}_{RL}^{\alpha_s}. \tag{7}$$

We notice that in the present theoretical framework the configuration averaging of a quantity simply reduces to the

evaluation of a particular matrix element in the enlarged augmented space. This theoretical result is *exact*. For numerical implementation this is the starting point for the various approximations such as the TCA and ICPA. We shall prefer to implement the recursion method of Haydock *et al.*[53] which is basically a transformation of the basis, through a three-term recurrence relation, to a new basis in which the Hamiltonian becomes tridiagonal and hence the diagonal part of averaged resolvent can be expressed as a continued fraction expansion involving the recursion coefficients a_n and b_n,

$$\langle\langle G(z)\rangle\rangle^{\alpha_s\alpha_s}_{RL,RL} = \cfrac{1}{z - a_1 - \cfrac{b_1^2}{z - a_2 - \cfrac{b_2^2}{z - a_3 - \cfrac{b_3^2}{\ddots}}}}.$$

Proper termination of the asymptotic part of this continued fraction constitutes the only approximation in the present theory, which retains the essential Herglotz analytic properties of the Green's function. Several terminators are available and we have chosen to use that of Beer and Pettifor.[54] Haydock[53] has carried out extensive studies of the errors involved and precise estimates are available in the literature. If we calculate the coefficients up to the nth step exactly, the first $2n$ moments of the density of states are reproduced exactly. This is a generalization of the method of moments, with the additional restriction that the asymptotically large moments are also accurately obtained.

Quantities required for self-consistent electronic-structure calculations such as charge densities, total densities of states, and total energies are all obtained from the projected density of states which are related to resolvents of the disordered system where one site in a sublattice (labeled R_0, α_s) is occupied by an atom of the type I,

$$\langle\langle G(z)\rangle\rangle^{\alpha_s(\mathbf{I})}_{R_0L_0,R_0L_0} = \langle\{\emptyset\} \otimes R_0\alpha_sL_0|(z\tilde{\mathbf{I}} - \tilde{\mathbf{H}}^{(2),(\mathbf{I})})^{-1}|\{\emptyset\} \otimes R_0\alpha_sL_0\rangle, \tag{8}$$

where

$$\tilde{\mathbf{H}}^{(2),(\mathbf{I})} = \tilde{\mathbf{H}}^{(1),(\mathbf{I})} - \tilde{\mathbf{h}}^{(\mathbf{I})}\tilde{\mathbf{o}}^{(\mathbf{I})}\tilde{\mathbf{h}}^{(\mathbf{I})}$$

and

$$\tilde{\mathbf{H}}^{(1),(\mathbf{I})} = \tilde{\mathbf{H}}^{(1)} + \tilde{\mathbf{C}}^{\alpha_s,(\mathbf{I})}_{R_0L_0} + (\tilde{\mathbf{\Delta}}^{\alpha_s,(\mathbf{I})}_{R_0L_0})^{1/2}\tilde{\mathbf{S}}(\tilde{\mathbf{\Delta}}^{\alpha_s,(\mathbf{I})}_{R_0L_0})^{1/2},$$

$$\tilde{\mathbf{h}}^{(\mathbf{I})} = \tilde{\mathbf{H}}^{(1),(\mathbf{I})} - \sum_{R\alpha_sL} \hat{\mathbf{E}}^{\alpha_s}_{\nu RL} \otimes \mathbf{P}^{\alpha_s}_{RL} - \tilde{\mathbf{E}}^{\alpha_s,(\mathbf{I})}_{\nu R_0L_0},$$

$$\tilde{\mathbf{o}}^{(\mathbf{I})} = \tilde{\mathbf{o}} + \tilde{\mathbf{o}}^{\alpha_s,(\mathbf{I})}_{R_0L_0},$$

where the various augmented potential parameters,

$$\tilde{\mathbf{X}}^{\alpha_s,(\mathbf{I})}_{R_0L_0} = (X^{\alpha_s,(\mathbf{I})}_{L_0}\hat{\mathbf{I}} - \hat{\mathbf{X}}^{\alpha_s}_{R_0L_0}) \otimes \mathbf{P}^{\alpha_s}_{R_0L_0}. \tag{9}$$

The projected density of states is obtained from

$$n^{\alpha_s,(\mathbf{I})}_{R_0}(E) = -\frac{1}{\pi}\Im m\sum_{L_0}\langle\langle G(E+i0^+)\rangle\rangle^{\alpha_s(\mathbf{I})}_{R_0L_0,R_0L_0}. \tag{10}$$

The total density of states in units of states/Ry atom is

$$n(E) = \frac{1}{N_{\text{cell}}}\sum_{\alpha_s}\sum_{R_0}\sum_{\mathbf{I}} x^{\alpha_s}_{\mathbf{I}} n^{\alpha_s,(\mathbf{I})}_{R_0}(E). \tag{11}$$

For our pseudobinary alloy $(A_{1-x}B_x)_3C$ in a tetragonally distorted face-centered-cubic lattice, there are two types of sublattices: α_1, the face-centered sites which are disordered and α_2, the cube-edge sites which are all occupied by C type of atoms. For α_1, $I=A$ or B, and $x^{\alpha_1}_B=x$ and $x^{\alpha_1}_A=1-x$. For a tetragonally distorted $L1_2$-type structure there are two types of atoms in the first sublattice, one at (110) (labeled α_{11}) and two identical ones at (101) and (011) (labeled α_{12}). While for α_2, $I=C$ and $x^{\alpha_2}_C=1$ and there is only one type of atom at $R_0=(000)$. The total number of atoms per unit cell $N_{\text{cell}}=4$. Thus

$$n(E) = \frac{1}{4}\{n^{\alpha_2,(C)}(E) + [xn^{\alpha_{11},(B)}(E) + (1-x)n^{\alpha_{11},(A)}(E)] + 2[xn^{\alpha_{12},(B)}(E) + (1-x)n^{\alpha_{12},(A)}(E)]\}. \tag{12}$$

At each concentration x, three separate augmented space recursions have been carried out with respect to three distinct maps corresponding to three inequivalent sites labeled by α_{11}, α_{12}, and α_2.

B. Phase stabilities

Our approach to the phases of the alloy will be from the point of view of stability. We shall start from a completely disordered alloy described by the occupation variables $\{n^{\alpha_s}_R\}$. The average $\langle\langle n^{\alpha_s}_R\rangle\rangle = x^{\alpha_s}_A$ for homogeneous perfect disorder. We then introduce fluctuations in the occupation variable at each site $\delta x^{\alpha_s}_R = n^{\alpha_s}_R - x^{\alpha_s}_A$. The generalized perturbation approach then expands the total internal energy in this configuration about the energy of the perfectly disordered state as

$$E = V^{(0)} + \sum_R\sum_{\alpha_s} V^{(1)}_{R\alpha_s}\delta x^{\alpha_s}_R + \sum_{RR'}\sum_{\alpha_s\alpha_{s'}} V^{(2)}_{R\alpha_s,R'\alpha_{s'}}\delta x^{\alpha_s}_R\delta x^{\alpha_{s'}}_{R'} + \cdots. \tag{13}$$

The coefficients $V^{(0)}$, $V^{(1)}_{R\alpha_s}$,…, are the effective renormalized cluster interactions. $V^{(0)}$ is the averaged total energy of the disordered medium. The "on-site energy" $V^{(1)}_{R\alpha_s}$ is unimportant for bulk ordered structures emerging from disorder. It is important for emergence of inhomogeneous disorder at surfaces and interfaces. The renormalized pair interactions $V^{(2)}_{R\alpha_s,R'\alpha_{s'}}$ are the most important quantities governing the emergence of bulk ordering. From Eq. (13) we may argue that the one body interaction $V^{(1)}_{R\alpha_s}$ is the energy difference between the situations when we immerse a B or an A atom in the disordered background at the site $R+\xi^{\alpha_s}$. In a homogeneously disordered situation this is independent of R. The pair interaction $V^{(2)}_{R\alpha_s,R'\alpha_{s'}}$ is the difference in one body interaction at $R+\xi^{\alpha_s}$ when site $R'+\xi^{\alpha_{s'}}$ is occupied either by an A or a B atom. These are given by

$$V^{(1)}_{R\alpha_s} = E^{A}_{R\alpha_s} - E^{B}_{R\alpha_s},$$

$$V^{(2)}_{R\alpha_s,R'\alpha_{s'}} = E^{AA}_{R\alpha_s,R'\alpha_{s'}} + E^{BB}_{R\alpha_s,R'\alpha_{s'}} - E^{AB}_{R\alpha_s,R'\alpha_{s'}} - E^{BA}_{R\alpha_s,R'\alpha_{s'}}, \tag{14}$$

where $E^{\mathbf{I}}_{R\alpha_s}$ is the total energy of random alloy with site $R+\xi^{\alpha_s}$ occupied by $\mathbf{I}=A$ or B type of atoms. $E^{\mathrm{IJ}}_{R\alpha_s,R'\alpha_{s'}}$ is the total energy of the random alloy with sites $R+\xi^{\alpha_s}$ and $R'+\xi^{\alpha_{s'}}$ occupied by I and J (both either A or B) types of atoms.

Since $V^{(1)}_{R\alpha_s}$ and $V^{(2)}_{R\alpha_s,R'\alpha_{s'}}$ are very small energy differences (on the order of millirydberg) of large energies (on the order of 10^3 Ry), a separate calculation of each component will produce errors larger than the small differences themselves. The orbital peeling method[51] based on recursion[55] was introduced by Burke precisely to calculate such small differences directly. The main points behind this method are described below.

The total energy of a solid may be separated into two parts: a one-electron band contribution E_{BS} and the electrostatic contribution E_{ES}. The renormalized cluster interactions defined in Eq. (13) should, in principle, include both of these contributions. However, since the cluster interactions involve the difference of cluster energies, it is usually assumed that the electrostatic terms cancel out, considering only the band-structure contribution to be important. Such an assumption is not rigorously true but it has been shown to be approximately valid in a number of alloy systems.[56] Considering only the band-structure contribution, the effective pair interactions (EPIs) can be calculated as follows.

The EPI can be related to the change in the configuration-averaged local density of states

$$V^{(2)}_{R\alpha_s,R'\alpha_{s'}} = \int_{-\infty}^{E_F} dE(E-E_F)\Delta N(E), \tag{15}$$

where $\Delta N(E)$ is given by

$$\Delta N(E) = -\frac{1}{\pi}\Im m\sum_{IJ}^{AB} \mathrm{Tr}\langle\langle(E\tilde{\mathbf{I}} - \tilde{\mathbf{H}}^{(\mathrm{IJ})})^{-1}\rangle\rangle\zeta_{IJ},$$

where $\zeta_{IJ}=2\delta_{IJ}-1$ and $\tilde{\mathbf{H}}^{(\mathrm{IJ})}$ is the augmented space Hamiltonian of a system where all sites except $R\alpha_s$ and $R'\alpha_{s'}$ are randomly occupied. These sites are occupied by atoms of the types I and J, respectively. The change in the averaged local density of states can be related to the generalized phase shift $\eta(E)$ through the following equation:

$$\Delta N(E) = \frac{d\eta(E)}{dE},$$

where $\eta(E)$ is given by

$$\eta(E) = \log\frac{\det\langle\langle\mathbf{G}^{AA}(E)\rangle\rangle\det\langle\langle\mathbf{G}^{BB}(E)\rangle\rangle}{\det\langle\langle\mathbf{G}^{AB}(E)\rangle\rangle\det\langle\langle\mathbf{G}^{BA}(E)\rangle\rangle}.$$

$\mathbf{G}^{\mathrm{IJ}}(E)$ is the resolvent of the augmented space Hamiltonian $\mathbf{H}^{(\mathrm{IJ})}$. The behavior of the above function is quite complicated and hence the integration [Eq. (15)] by standard routines is difficult. Furthermore, the integrand is multivalued, being simply the phase of $\Sigma_{\mathrm{IJ}}\det(\mathbf{G}^{\mathrm{IJ}})\zeta_{\mathrm{IJ}}$. The way out of this was suggested by Burke,[51] who gave an elegant way of calculating the phase shift $\eta(E)$ following the orbital peeling method. The method basically relies on the repeated application of the downfolding theorem on the Hamiltonian $\mathbf{H}^{(\mathrm{IJ})}$. We shall quote only the final result. The pair energy function is defined as

$$\begin{aligned} f_{R\alpha_s,R'\alpha_{s'}}(E) &= \sum_{\mathrm{IJ}}^{AB}\sum_{k=1}^{\ell_{\max}}\zeta_{\mathrm{IJ}}\int_{-\infty}^{E} dE'(E'-E)\log\langle\langle\mathbf{G}^{\mathrm{IJ}}_k(E')\rangle\rangle \\ &= 2\sum_{\mathrm{IJ}}^{AB}\sum_{k=1}^{\ell_{\max}}\left[\sum_{m=1}^{z^{k,\mathrm{IJ}}} Z^{k,\mathrm{IJ}}_m - \sum_{m=1}^{p^{k,\mathrm{IJ}}} P^{k,\mathrm{IJ}}_m + (p^{k,\mathrm{IJ}} - z^{k,\mathrm{IJ}})E\right], \end{aligned} \tag{16}$$

where $\langle\langle\mathbf{G}^{\mathrm{IJ}}_k(E)\rangle\rangle$ denote the configuration-averaged resolvents of the disordered Hamiltonian with occupancy at sites $R\alpha_s$ and $R'\alpha_{s'}$ by I and J types of atoms, of which the projected orbitals 1 to $k-1$ have been deleted (peeled). $Z^{k,\mathrm{IJ}}_m$ and $P^{k,\mathrm{IJ}}_m$ are its zeros and poles and $z^{k,\mathrm{IJ}}$ and $p^{k,\mathrm{IJ}}$ are the number of such zeros and poles below E. The zeros and poles are obtained directly from the recursion coefficients of the averaged resolvents and these are obtained from the TB-LMTO-ASR. The effective pair interaction is then given by

$$V^{(2)}_{R\alpha_s,R'\alpha_{s'}} = f_{R\alpha_s,R'\alpha_{s'}}(E_F). \tag{17}$$

If ordering in only a given sublattice is considered then the quantity required is $V^{(2)}_{R\alpha_s,R'\alpha_s}$. This is relevant for our example $(A_{1-x}B_x)C$, where the α_1 sublattice sites are not random and ordering takes place only in the α_2 sublattice. The general formulation also can tackle ordering across different sublattices.

In what follows we shall specialize to our given pseudobinary problem where ordering takes place only in one of the sublattices. It has been noticed that a wide range of phenomena related to order-disorder transitions can be explained using the symmetry properties of the pair interactions $V^{(2)}_{R\alpha_s,R'\alpha_s}$. The study of phase stability requires reliable approximations to the configurational energy as well as the use of statistical models to obtain the configurational entropy. The configurational energy within the pair interaction can be represented in Fourier space as the product of the Fourier transform of the effective pair interaction $V(\mathbf{k})$ and that of the pair-correlation function $Q(\mathbf{k})$,

$$E \simeq \frac{N}{2}\sum_{\mathbf{k}} V(\mathbf{k})Q(\mathbf{k}),$$

where N is the number of atoms. Minimization of E will naturally occur for states of order characterized by maxima in the $Q(\mathbf{k})$ pair-correlation spectrum located in regions of the absolute minima of $V(\mathbf{k})$. Consequently, much can be predicted about the types of ordering to be expected from a study of the shape of $V(\mathbf{k})$, particularly from a search of its absolute minima $\mathbf{h}$ (called special points). At these special

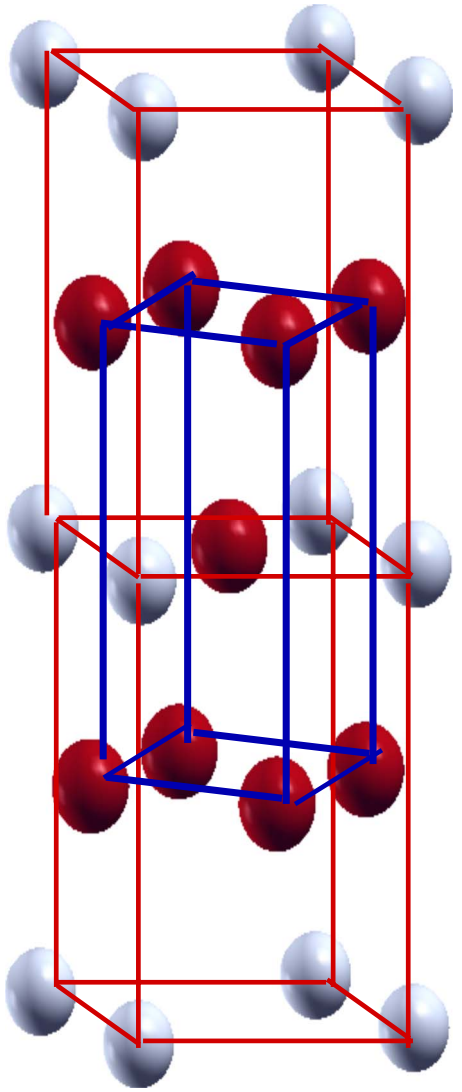

FIG. 2. (Color online) Interpenetrating tetragonal and body-centered tetragonal lattices make up the larger face-centered tetragonal lattice. Al atoms on the outer tetragonal lattice are shown as (cyan) gray while the Ni(Pt) atoms in the inner body-centered tetragonal disordered lattice is shown as (magenta) dark spheres.

points, $|\nabla_{\mathbf{h}} V(\mathbf{h})|=0$. These special points are always located at the surface of Brillouin zone. The *star* of a special point vector **k** is obtained by applying all the rotations and rotation inversions of the space group on the vector **k**. All these vectors of a star are considered equivalent.

We note first that the sublattice on which the disorder is taking place is a body-centered tetragonal (bct) lattice embedded in the larger face-centered tetragonal lattice. This is clear from Fig. 2. The special points of the bct structure are located at the points Γ, H, and R of the Brillouin zone. Minima of $V(\mathbf{k})$ at these points predict various kinds of ordered structures that could be obtained by the superposition of concentration waves for equivalent points corresponding to a single star. A minimum at the Γ point, $\mathbf{h}=[000]$, indicates phase separation while a minimum at the point H, $\mathbf{h}=[100]$ in the bct lattice suggests B2-type ordering.

We have investigated the stability of the ordered structures in the bct-based sublattice in the pseudobinary alloy $(A_{1-x}B_x)C$ based on these concepts of the lattice Fourier-transformed effective pair interactions. Once the pair interaction energies have been calculated, they may be used for the calculation of the mixing enthalpy, ordering energy, instability temperature, and the short-range order maps to predict the most stable superordered structures.

With reference to the total energies of the pure constituents, in the approximation where we only restrict ourselves to pair energies and ignore all three body interactions and higher, the so-called mixing enthalpy is defined as

$$E_{\text{mix}} = -\frac{1}{2}x(1-x)\sum_n V_{0n}^{(2)} N_n. \tag{18}$$

The generalized perturbation method[56] defines an ordering energy as

$$E_{\text{ord}} = \frac{1}{2}x\sum_n V_{0n}^{(2)}(N_n^{BB} - xN_n), \tag{19}$$

where in the given ordered structure, n is the nth nearest neighbor of an arbitrarily chosen site (which we label 0), N_n^{BB} is the number of BB pairs, and N_n is the total number of pairs in the nth nearest-neighbor shell of 0.

The expressions for mixing and ordering energies, calculated in terms of pair potentials considering up to fourth nearest neighbors for $x=1/3$ and 2/3 concentrations of Pt in $(Ni_{1-x}Pt_x)_3Al$ pseudobinary alloy are then given by

$$E_{\text{mix}}\left(x=\frac{1}{3}\right) = -\frac{2}{9}(4V_1 + 2V_2 + V_3 + 8V_4),$$

$$E_{\text{mix}}\left(x=\frac{2}{3}\right) = -\frac{2}{9}(2V_1 + 2V_2 + V_3 + 2V_4),$$

$$E_{\text{ord}}\left(x=\frac{1}{3}\right) = -\frac{1}{9}(4V_1 - 4V_2 - 2V_3 + 8V_4),$$

$$E_{\text{ord}}\left(x=\frac{2}{3}\right) = -\frac{1}{9}(8V_1 - 4V_2 - 2V_3 - 4V_4), \tag{20}$$

where V_n are the effective pair interaction for the nth nearest neighbor.

A sufficient (but not necessary) condition, formally shown by Clapp and Moss,[57] for a stable ground state is that the wave vector of concentration waves corresponding to an ordered phase lie in the positions of the minima of the Fourier transform of the pair energy function: $V(\mathbf{k})$. The Krivoglatz-Clapp-Moss short-range order parameter related to the diffuse scattering intensity is defined as

$$\alpha(\mathbf{k}) = \frac{C}{1 + x(1-x)\beta V_{\text{ren}}(\mathbf{k})}, \tag{21}$$

where

$$\frac{1}{C} = \int \frac{d\mathbf{k}}{8\pi^3} \frac{1}{1 + x(1-x)\beta V_{\text{ren}}(\mathbf{k})}.$$

The ring approximation in the grand-canonical ensemble described by Chepulskii and Bugaev,[58] expresses the renormalized pair function V_{ren} as

$$V_{\text{ren}}(\mathbf{k}) = V(\mathbf{k}) - \frac{\beta}{2}(1-2x)^2 \int \frac{d\mathbf{q}}{8\pi^3} F(\mathbf{q}) F(\mathbf{k}-\mathbf{q}), \quad (22)$$

where

$$F(\mathbf{q}) = \frac{V(\mathbf{q})}{1 + x(1-x)\beta V(\mathbf{q})}.$$

It is straightforward to show that the minima of the pair-function $V_{\text{ren}}(\mathbf{k})$ coincide with the maxima of the diffuse scattering intensity.

We have further used Khachaturian's concentration wave approach in which the stability of a solid solution with respect to a small concentration wave of given wave vector $\mathbf{k}$ is guaranteed as long as $k_B T + V(\mathbf{k})x(1-x) > 0$. Instability of the disordered state sets in when

$$k_B T^i + V_{\min} x(1-x) = 0, \quad (23)$$

where T^i is the instability temperature corresponding to a given concentration wave disturbance. $V_{\min}$ is the absolute minima in the effective pair potential surface and x is the concentration of one of the constituent atoms.

III. RESULTS AND DISCUSSION

A. Computational details

One of the difficulties associated with the TB-LMTO-ASR method is the enormous rank of the enlarged augmented space. The rank of this Hilbert space for a pseudobinary alloy is $(N_d \times 2^{N_d} + N_o)$ for a system of $N_{tot} = N_d + N_o$ lattice sites with binary distribution (with respect to A and B type of atoms) on N_d number of sites and N_o number of sites with fixed occupancy by the C type of atom. In an earlier communication[59] we have discussed how one may use the local symmetries of the augmented space to reduce the rank of the Hamiltonian and carry out the recursion on a reducible subspace of much lower rank. In case of pair interaction calculation if we fix the occupation of two sites (Ith and Jth sites), the local symmetry of the augmented space is further lowered. We may then carry out the recursion in a suitably reduced space.

For our calculations, the real-space clusters were generated out of 2000–2500 atoms, which gave rise to about 1 700 000 states in the enlarged augmented space, consisting of both real-space and configuration-space labelings. Each atom in the real-space cluster has 18 neighbors (nearest and next nearest) around it and hence yields a pretty good coverage of the far environment around each site. 12 steps of recursion were carried out and the continued fraction terminated by the Beer and Pettifor terminator.[54] This gave the configuration-averaged Green's function. The same number of recursion steps was used for the pair interaction OP calculation.

As already mentioned, in order to check the reliability of our computational method and to answer the questions regarding the stability of superordered structures in pseudobinary alloys, we have chosen the face-centered tetragonal-based $(Ni_{1-x}Pt_x)_3Al$ alloy system. Though, the parent compounds, NiPt and NiAl alloys, have been extensively studied[32,47,49,50] in the past, there exist very few theoretical investigations (see Jiang *et al.*,[46] and references therein) of pseudobinary compounds based on these binary alloys.

First of all we shall show the effectiveness of the TB-LMTO-ASR method by calculating the alloy density of states and hence the Fermi energy, which is the most crucial quantity for an accurate calculation of pair interaction energy, at two different concentrations of Pt, $x = 1/3$ and 2/3. The phase stability search is then carried out using the orbital peeling method within the framework of ASR for the calculation of the effective pair potentials described at length in the earlier section. The results obtained were compared with the existing theoretical results available in the literature. The calculations were performed both nonrelativistically as well as scalar relativistically and the exchange-correlation potential of Von Barth and Hedin was used. In an earlier communication,[32] we have shown that the calculations done with the same Wigner-Seitz radius (charged spheres) for the constituent atoms in an alloy leads to unphysical results. However following the procedure described by Kudronovský and Drchal,[60] which is an extension of the procedure proposed by Andersen and Jepsen,[22] one can make choices of the atomic sphere approximated (ASA) radii for the constituents, which is capable of taking into account charge self-consistency in a reasonable manner. The idea is to choose ASA radii of atomic species in such a way that the spheres are charge neutral on average. We have utilized this procedure throughout our calculation to correctly take into account the charge-transfer effect which is one of the most important factor in any electronic-structure calculation.

Of the two concentrations, the c/a ratio for $x = 1/3$ and 2/3 are 1.02 and 0.92, respectively. The equilibrium lattice parameters are given by $a = 3.67$ Å and $c = 3.74$ Å for $x = 1/3$ and $a = 3.93$ Å and $c = 3.616$ Å for $x = 2/3$. These equilibrium lattice parameters were obtained by minimizing the total DFT energies with respect to the lattice parameters. These structural parameters compare quite well with those of the existing theoretical and experimental findings.[42,43,46]

Pt being one of the constituents, one would expect relativistic effects to be important. For the stabilization of the NiPt alloy system, relativistic effect has been found to play a crucial role.[32,35] It is of interest therefore, to find out whether such a dependence extends also to case of pseudobinary alloys $(Ni_{1-x}Pt_x)_3Al$. For this purpose, we have carried out calculations considering the nonrelativistic form of the Hamiltonian also.

B. Results of nonrelativistic calculations

In Table I we show the ordering energy and the mixing energy of the $(Ni_{1-x}Pt_x)_3Al$ alloy for Pt concentration $x = 1/3$ and 2/3, without including the relativistic corrections to the Hamiltonian. These energies are calculated from Eqs. (18) and (19), respectively.

TABLE I. Mixing and ordering energies (in mRy/atom) for the two compositions in $(Ni_{1-x}Pt_x)_3Al$ alloy with nonrelativistic calculations.

Composition	E_{mix}	E_{ord}
$x=1/3$	0.20	−0.15
$x=2/3$	1.21	1.80

One can easily notice from Table I that the mixing energy for the composition $x=1/3$ come out to be positive and the ordering energy is very small negative indicating an overall tendency to segregate. Moreover, both these energies are positive for $x=2/3$ indicating an overwhelming segregating tendency. Both these contradict experimental observation. These results reflect the inadequacy of the nonrelativistic Hamiltonian to describe the problem of phase stability in this class of pseudobinary alloys and confirms the importance of the relativistic effects to the Hamiltonian. Keeping in mind that the pair interactions have magnitude approximately a few mRy/atom and they are sensitive to changes in the Hamiltonian, we carry out all the calculations with the scalar-relativistic form of the TB-LMTO Hamiltonian which includes mass-velocity and Darwin terms.

C. Results of scalar-relativistic calculations

Figure 3 shows the projected and total DOS at the alloy compositions $x=1/3$ and 2/3 and compares them with the ordered Ni_2PtAl and $NiPt_2Al$, respectively. In both the panels the quadrants show the projected DOS for Al, Ni, and Pt with the total DOS all in units of states/Ry cell. The left quadrants

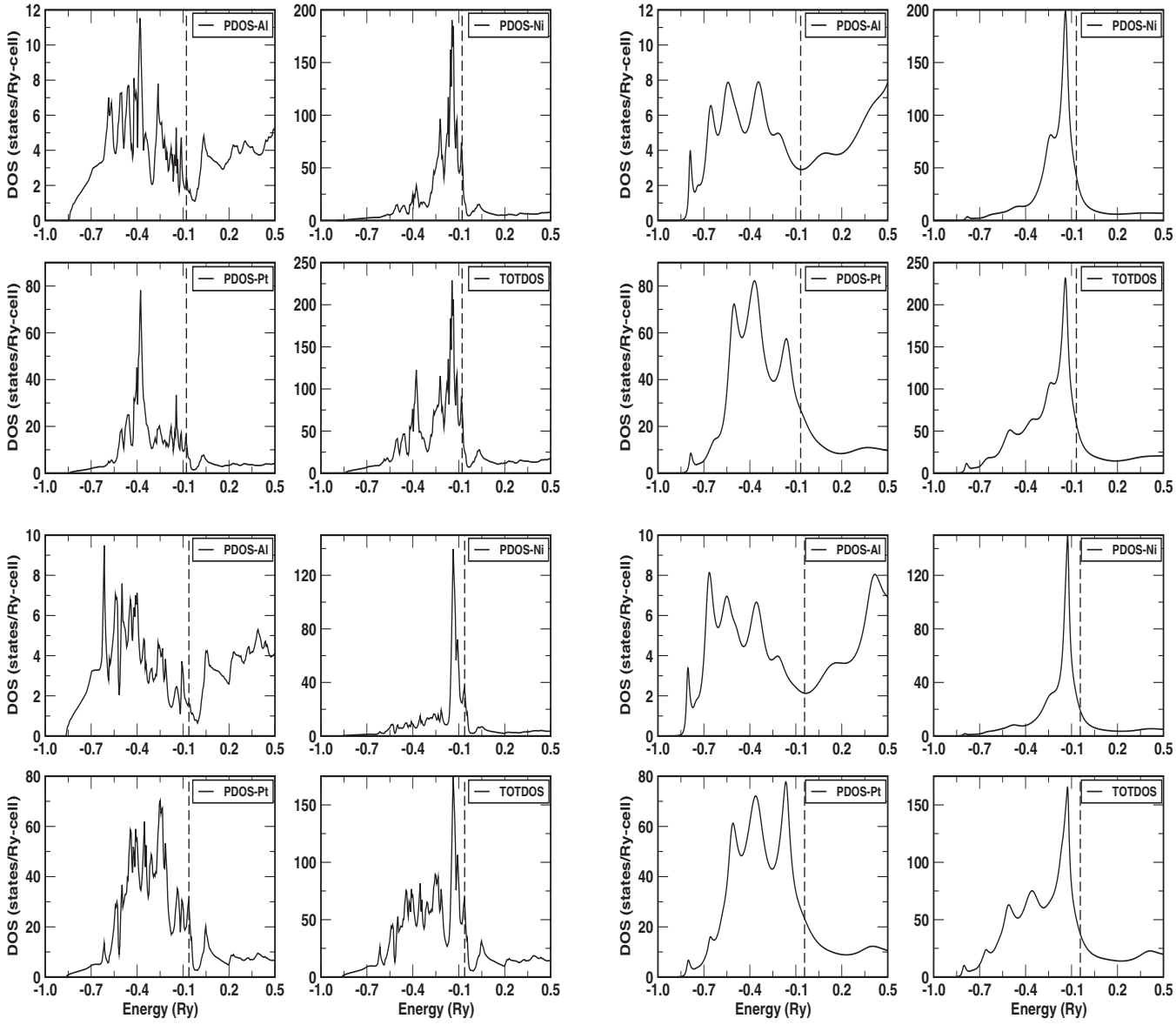

FIG. 3. (Top panel) Partial and total densities of states for (left quadrant) ordered Ni_2PtAl (right quadrant) disordered $(Ni_{1-x}Pt_x)_3Al$ with $x=1/3$. (Bottom panel) Partial and total densities of states for (left quadrant) ordered $NiPt_2Al$ (right quadrant) disordered $(Ni_{1-x}Pt_x)_3Al$ with $x=2/3$. Note the change in scale of the y axis between Al, Ni, and Pt partial DOS.

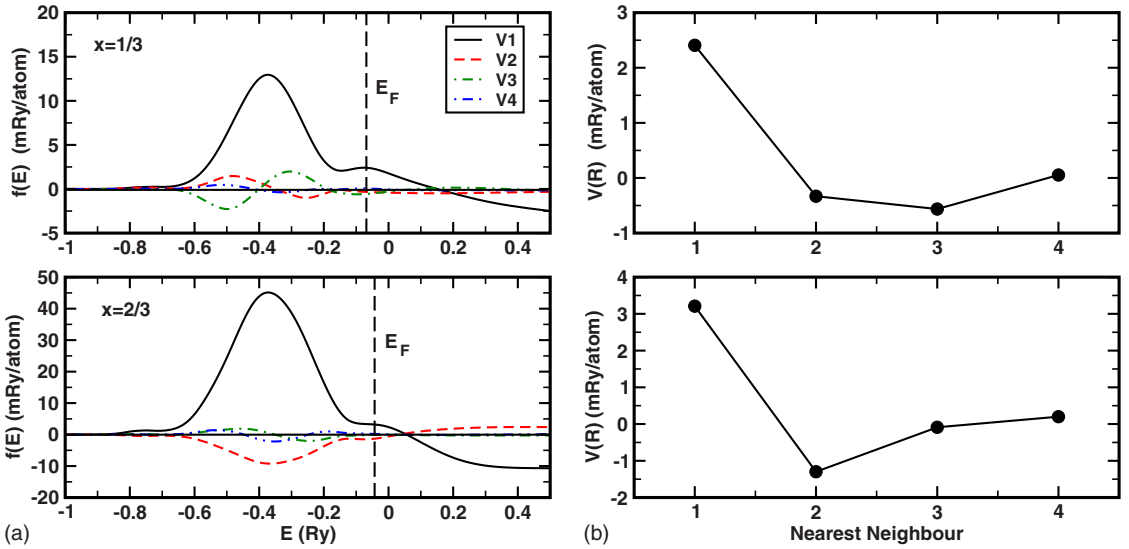

FIG. 4. (Color online) (Left panel) The real-space functions $f(E)$ [Eq. (16)] plotted as functions of energy for $(Ni_{1-x}Pt_x)_3Al$ alloys: $x=1/3$ and 2/3. The solid (black), dashed (red), dot-dashed (green), and long-dashed (blue) lines in the two panels indicate the pair functions $f(E)$ between the first (V_1), second (V_2), third (V_3), and fourth (V_4) neighboring atoms. The vertical dashed line indicates the alloy Fermi level. (Right panel) The actual effective pair interactions [Eq. (17)].

are for the ordered and the right ones for the disordered alloys. E_F is indicated by the vertical dashed lines.

The first thing to note is that for the partial DOS for Al and Ni for both the compositions, the disordered and ordered DOS structures are not very different from each other. The disordered structures are, of course, broadened by disorder scattering. There is some rearrangement of structures for the partial DOS for Pt, particularly for $x=1/3$. The Al partial DOS contributed by Al *s* and *p* bands are much broader compared to Pt *d* and Ni *d* dominated partial DOS of Pt and Ni. Contributions from Pt *s* and *p* bands can be noticed near the band edge. The total DOS for both the compositions resemble each other quite closely. This indicates that although there has been considerable charge-transfer effects when we alloy the constituents, there is only a small *extra* charge transfer when we go from the ordered to the disordered phase. The Fermi level E_F shifts only slightly with composition.

We shall now discuss the phase stability of the two alloys. It will be shown that how the inclusion of relativistic corrections and a reasonable choice of the Wigner-Seitz radius of the constituents (to maintain charge neutrality) help to predict the stability of the correct phase at all concentration range. Figure 4 shows the EPI for two $(Ni_{1-x}Pt_x)_3Al$ pseudobinary alloys within the bct structure on which ordering takes place. These pair energies are calculated only with respect to the interactions between the disordered constituents Ni and Pt. Al atoms are kept fixed at the cube corners, so do not participate in the ordering process. The top and the bottom panels of Fig. 4 show the pair energy functions for concentrations $x=1/3$ and 2/3, respectively. The solid, dashed, dot-dashed, and long-dashed lines show the pair interaction energies between the first (V_1), second (V_2), third (V_3), and fourth (V_4) nearest-neighboring atoms. There are some common features which both the alloys share. As for instance, the magnitude of first neighboring pair interaction (V_1) is always greater than the other more distant neighboring pair energies. The pair energies rapidly converge to zero with distance. In fact, we have shown the pair energies up to the fourth-nearest-neighbor shell and we have checked that the magnitude of the pair energies beyond fourth shell are smaller than the error bars of our calculational method and therefore these numbers are not really reliable. We have therefore calculated the ordering and mixing energies with contributions only up to the fourth neighboring shell. The very first thing we note from Fig. 4 is the positive sign of V_1, which predicts an ordering behavior for both the alloys.

Based on these real-space pair interaction energies, we have then estimated the ordering and the mixing energies for the two alloy systems as shown in Table II. Unlike the results shown in Table I, where the ordering and mixing energies for composition $x=2/3$ were positive, with relativistic corrections these energies are now negative for both compositions and hence favor ordering as predicted by other theories[46] and experiments.[42,43] This shows that the scalar-relativistic effects play an important role in predicting the correct ground state.

A quantitative comparison of our mixing enthalpies with that of the cluster expansion (CE) and the SQS results[46] for two alloy compositions are shown in Table III. It is easy to notice that our results obtained with the inclusion of relativ-

TABLE II. Mixing and ordering energies (in mRy/atom) for the two compositions in $(Ni_{1-x}Pt_x)_3Al$ alloy with scalar-relativistic calculations.

Composition	E_{mix}	E_{ord}
$x=1/3$	−1.96	−1.39
$x=2/3$	−0.92	−3.36

TABLE III. Formation enthalpies (in eV/formula unit) for fcc-based pseudobinary $(Ni_{1-x}Pt_x)_3Al$ alloys with the choice of charge neutral spheres including the scalar-relativistic corrections. The values within brackets are without relativistic correction. The third and fourth columns correspond to the results obtained form the cluster expansion and the SQS calculation of Ref. 46.

Composition	This work SR (NR)	CE (Ref. 46)	SQS (Ref. 46)
$x=1/3$	−0.100 (+0.011)	−0.065	−0.068
$x=2/3$	−0.055 (+0.066)	−0.072	−0.090

istic corrections are in closer agreement with other results.

We need also to predict which type of superstructure is stable. Figure 5 shows three possible ordered arrangements for Ni_2PtAl. We can obtain the energy difference between these structures using the pair energies. The leftmost layered structure has the minimum energy. On the face-centered tetragonal lattice it is a type of $L1_0$ structure with Ni in layers capped by Pt. On the underlying bct lattice on which ordering takes place this is a B2 like arrangement. The energy of the middle structure is merely 0.05 mRy/atom higher for the $x=1/3$ composition and 8.0 mRy/atom higher for the $x=2/3$ composition. This is also a layered structure with alternating Ni and Pt layers capped with Ni. The third structure to the far right is higher in energy still. Recently there has been theoretical predictions by Jiang *et al.*[46] as well as experimental work by Kamm and Milligan,[42] and Meininger and Ellner[43] both of which predict $L1_0$ or layered type ordering on the face-centered tetragonal lattice (equivalently B2 ordering on the embedded bct lattice) at $x=2/3$ composition.

In order to reconfirm the stability of a specific type of superordered structure at the two extreme end concentration range, we have followed an alternative path via calculating the Fourier transform $V(\mathbf{k})$ of the real-space pair energies and analyze the minima of this effective potential surface. Figure 6 shows the effective pair potential surface $V(\mathbf{k})$ on (left panels) the $k_z=0$ plane and (right panels) the plane bounded by (001) and (110) lines for the $(Ni_{1-x}Pt_x)_3Al$ alloys. The top and bottom panels show the pair potential surfaces for $x=1/3$ and 2/3 compositions. Each of these plots has a minima at the special point $\langle \mathbf{100} \rangle$. In the bct sublattice this indicates a B2 ordering. A look at Fig. 2 convinces us that this indicates a $L1_0$-based structure in the full fcc-based lattice at $x=1/3$ and 2/3. The $x=1/3$ case has a shallow dip at $(\frac{1}{2},\frac{1}{2},\frac{1}{2})$ while the $x=2/3$ case has a saddle point there. This has no bearing on the prediction of the stability of the $L1_0$ (B2) like structure but will bear upon the path taken to transition from disorder to ordering across the instability temperature (Table IV).

A quantitative evaluation of the minima of these pair potential surface yields an estimate of the order-disorder transition temperature. Once these minima are located, the instability temperature T^i can then be evaluated from Eq. (23). The instability temperatures are ~1027 and ~1379 K for the alloys $x=1/3$ and 2/3, respectively. It should be noted that the transition temperature of $L1_0Ni_2PtAl$ $(x=1/3)$ is comparatively lower than that for $x=2/3$. A very recent theoretical investigation[46] of this alloy system predicts the order-disorder transition temperature for $L1_0$ Ni_2PtAl to be ~915 K. The experimental order-disorder transition temperature for the $x=2/3$ composition is 1423 K. We have slightly underestimated this in our phase stability study via the orbital peeling calculation. The discrepancy is however quite small and its possible reason is the neglect of the effects of nonconfigurational (vibrational, electronic, etc.) entropies in our calculation which might cause a shift of the order-disorder transition temperatures.

The SRO "parameters" $\alpha(\mathbf{k})$ are the most sensitive quantities to approximation in the study of disordered alloys. We have estimated these parameters for different ordering stars

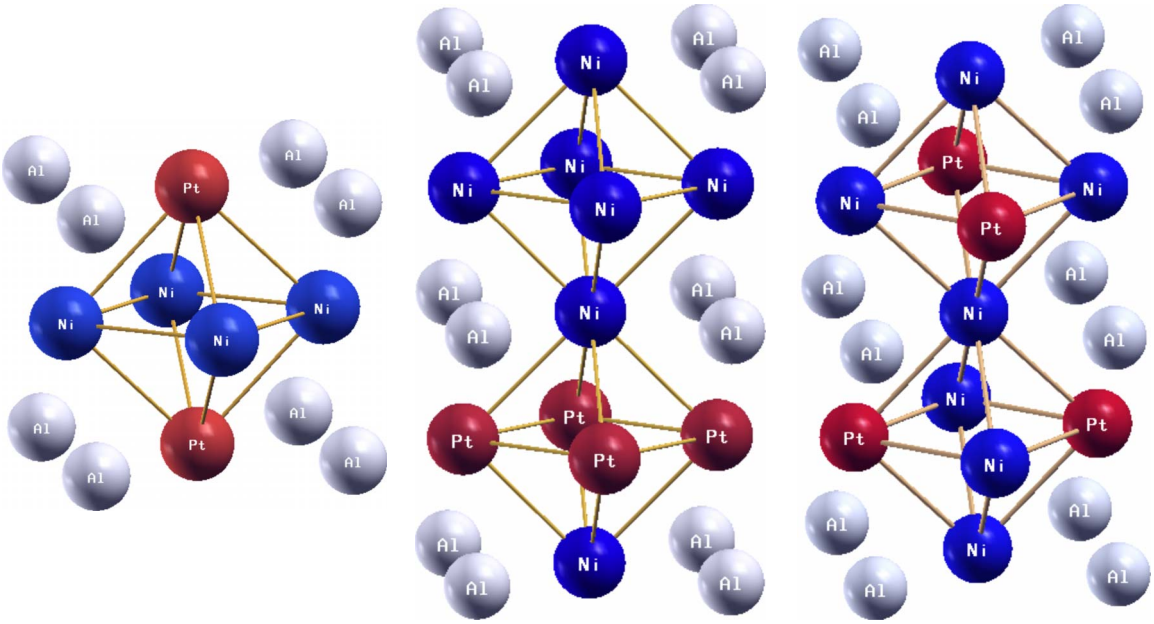

FIG. 5. (Color online) Three possible ordered structures of the type Ni_2PtAl. Similar structures are possible for $NiPt_2Al$. One can go from one to the other by simply interchanging Ni and Pt atoms.

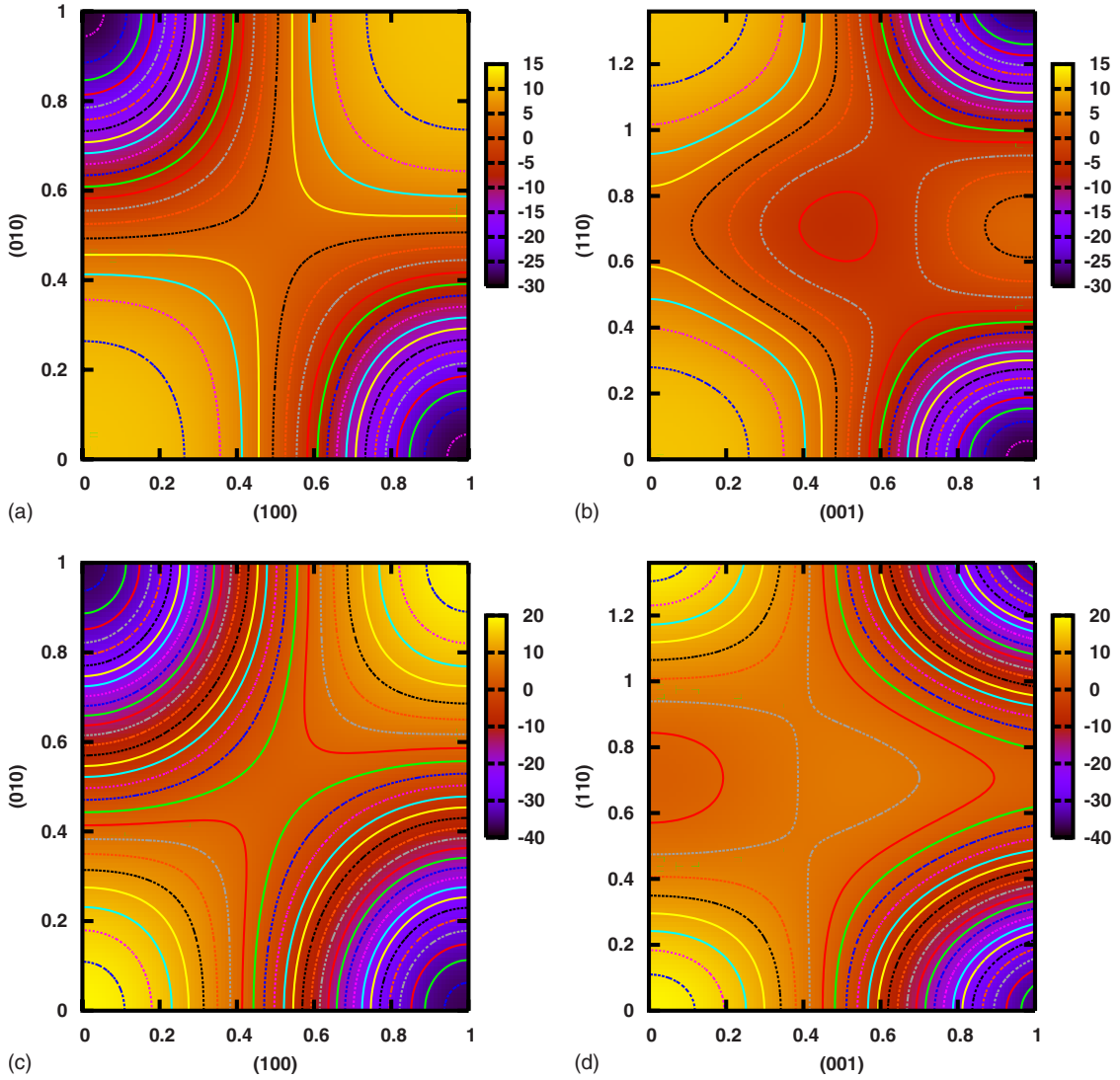

FIG. 6. (Color online) The effective pair potential surface $V(\mathbf{k})$ in reciprocal space projected on the plane bounded by (left panels) (100) and (010) axes and (right panels) (001) and (110) axes, for the $(Ni_{1-x}Pt_x)_3Al$ alloy. The top and bottom panels correspond to $x=1/3$ and 2/3 alloy compositions. These results were calculated with the choice of charge neutral spheres including the scalar-relativistic correction to the Hamiltonian into account.

using the pair interaction energies for $(Ni_{1-x}Pt_x)_3Al$ alloys at one of the compositions ($x=2/3$). The results are shown in Fig. 7. These SRO functions were calculated at intervals of 1.6 K up to about 10 K above the instability temperature, using the above explained first four nearest-neighbor pair interaction energies, to see the effect of SRO in the disordered phase. These SRO values show peak positions at the special points $\langle\mathbf{100}\rangle$. These peak positions correspond to the diffused scattering peaks which clearly show the $L1_0$-type (B2 on the ordering lattice) short-range ordering for the $x=2/3$ concentration of Pt in the disordered phase of these alloy systems. The SRO function clearly develops peaks at the special points (100) and (010) as we approach the transition temperature from above. This confirms the transition from the disordered to the $L1_0$-type (B2) phase.

TABLE IV. Minima of the effective pair potential $V\langle\mathbf{hkl}\rangle$ surface for the fcc-based pseudobinary $(Ni_{1-x}Pt_x)_3Al$ alloys.

Alloy composition	Experimental ordering	$\mathbf{V}_{\mathbf{min}}$
$x=1/3$	$\langle\mathbf{100}\rangle$ B2	−29.29
$x=2/3$	$\langle\mathbf{100}\rangle$ B2	−39.32

IV. CONCLUSION

The aim of this work was to introduce and examine the suitability and accuracy of the ASR-based orbital peeling (OP) method for the phase stability study of the pseudobinary alloys. We have applied the developed technique to $(Ni_{1-x}Pt_x)_3Al$ pseudobinary alloys. Our analysis shows that for the phase stability study, it is essential to take into account both the relativistic corrections and the proper handling of the effects of charge transfer by a choice of the charge neutral spheres. Our ground state search identified

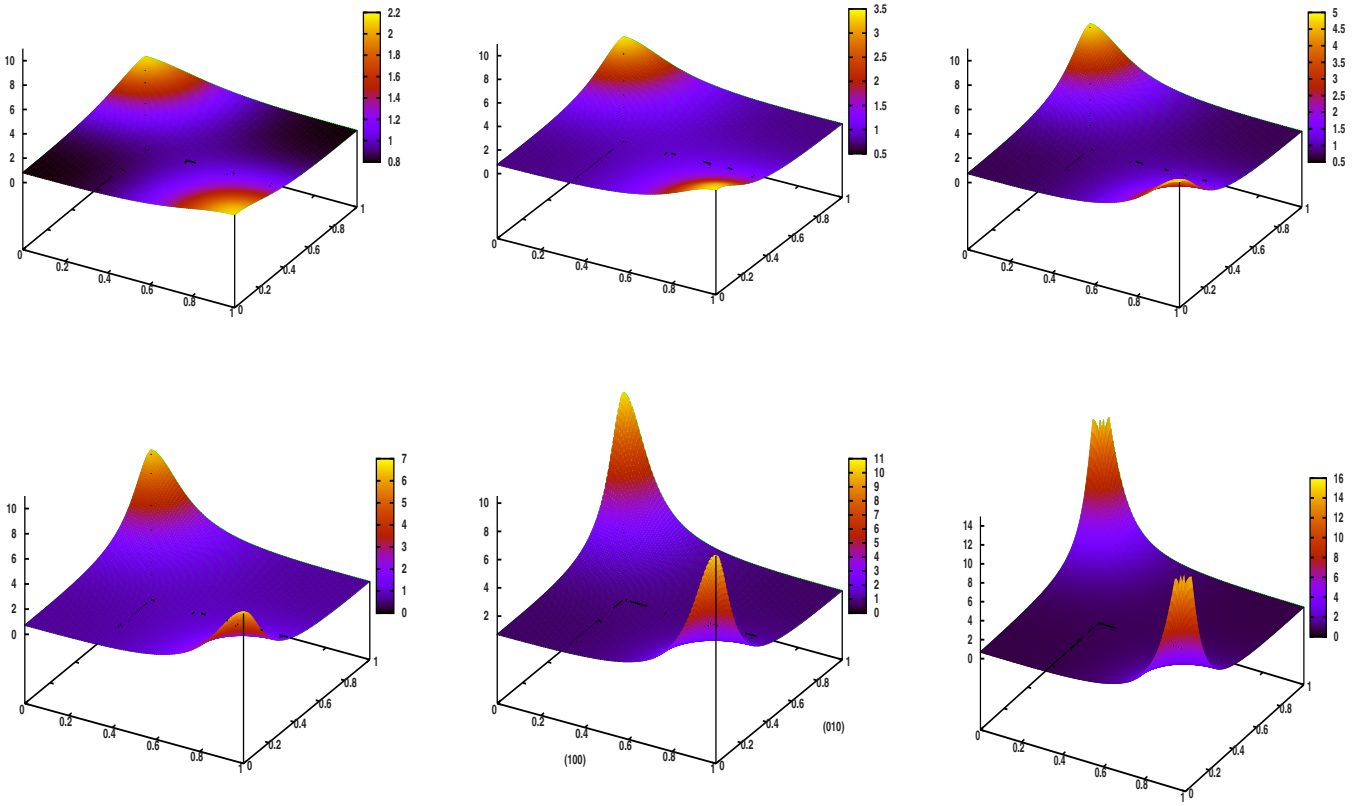

FIG. 7. (Color online) The reciprocal space SRO surfaces $\alpha(\mathbf{k})$ on $k_z=0$ plane for the $(Ni_{1-x}Pt_x)_3Al$ alloy at different temperatures above the instability temperature. The development of peaks at (100) and (010) special points is clearly shown. This corresponds to $x=2/3$ alloy composition. These results were calculated using the ring approximation.

$L1_0$ (B2) type structures for both Ni_2PtAl and $NiPt_2Al$. The latter has been observed experimentally. Our computed instability temperatures are in fair agreement with both earlier theoretical approaches as well as the experimental findings. We have also compared our calculated mixing enthalpies with earlier results. We have further calculated the short-range order maps which may be compared with future experimental measurements. Based on the success of our test case, we propose the ASR technique as a computationally efficient method for the electronic structure and phase stability studies of multicomponent and multisublattice alloys with varying nature of disorder on different sublattices. This case study will form the basis of further studies on these systems.

ACKNOWLEDGMENTS

One of the authors (A.A.) would like to acknowledge financial support from the Department of Energy (Grant No. DEFG02-03ER46026) and Lawrence Livermore National Laboratory (Grant No. B573247) during the time this work was done. T.S.D. and A.M. acknowledge the computational facility of Advanced Materials Research Unit (AMRU).

[1] G. M. Stocks, W. M. Temmerman, and B. L. Gyorffy, Phys. Rev. Lett. **41**, 339 (1978).
[2] P. Soven, Phys. Rev. **156**, 809 (1967).
[3] E. G. Moroni and T. Jarlborg, Phys. Rev. B **47**, 3255 (1993).
[4] D. J. Singh, J. Appl. Phys. **76**, 6688 (1994).
[5] M. H. F. Sluiter, K. Esfarjani, and Y. Kawazoe, Phys. Rev. Lett. **75**, 3142 (1995).
[6] G. Moraitis, M. A. Khan, H. Dreysee, and C. Demangeat, J. Magn. Magn. Mater. **156**, 250 (1996).
[7] P. Olsson, I. A. Abrikosov, and J. Wallenius, Phys. Rev. B **73**, 104416 (2006).
[8] A. Zunger, S.-H. Wei, L. G. Ferreira, and J. E. Bernard, Phys. Rev. Lett. **65**, 353 (1990).
[9] Y. Wang, G. M. Stocks, W. A. Shelton, D. M. C. Nicholson, Z. Szotek, and W. M. Temmerman, Phys. Rev. Lett. **75**, 2867 (1995).
[10] I. A. Abrikosov, S. I. Simak, B. Johansson, A. V. Ruban, and H. L. Skriver, Phys. Rev. B **56**, 9319 (1997).
[11] M. Jarrell and H. R. Krishnamurthy, Phys. Rev. B **63**, 125102 (2001).
[12] D. A. Rowlands, J. B. Staunton, B. L. Gyorffy, E. Bruno, and B. Ginatempo, Phys. Rev. B **72**, 045101 (2005).
[13] D. D. Johnson, D. M. Nicholson, F. J. Pinski, B. L. Gyorffy, and G. M. Stocks, Phys. Rev. B **41**, 9701 (1990).

[14] R. Mills and P. Ratanavararaksa, Phys. Rev. B **18**, 5291 (1978).
[15] T. Kaplan and M. Mostoller, Phys. Rev. B **9**, 1783 (1974).
[16] H. W. Diehl, P. L. Leath, and T. Kaplan, Phys. Rev. B **19**, 5044 (1979).
[17] T. Kaplan, P. L. Leath, L. J. Gray, and H. W. Diehl, Phys. Rev. B **21**, 4230 (1980).
[18] S. Ghosh, P. L. Leath, and M. H. Cohen, Phys. Rev. B **66**, 214206 (2002).
[19] T. Saha, I. Dasgupta, and A. Mookerjee, J. Phys.: Condens. Matter **6**, L245 (1994).
[20] A. Mookerjee, J. Phys. C **6**, L205 (1973).
[21] A. Mookerjee, J. Phys. C **6**, 1340 (1973).
[22] O. K. Andersen and O. Jepsen, Phys. Rev. Lett. **53**, 2571 (1984).
[23] T. Saha and A. Mookerjee, J. Phys.: Condens. Matter **8**, 2915 (1996).
[24] T. Saha, I. Dasgupta, and A. Mookerjee, Phys. Rev. B **50**, 13267 (1994).
[25] A. Alam and A. Mookerjee, J. Phys.: Condens. Matter **21**, 195503 (2009).
[26] A. Mookerjee and R. Prasad, Phys. Rev. B **48**, 17724 (1993).
[27] A. Alam, S. Ghosh, and A. Mookerjee, Phys. Rev. B **75**, 134202 (2007).
[28] K. Tarafder, A. Chakrabarti, K. K. Saha, and A. Mookerjee, Phys. Rev. B **74**, 144204 (2006).
[29] A. Alam and A. Mookerjee, Phys. Rev. B **72**, 214207 (2005).
[30] T. Saha and A. Mookerjee, J. Phys.: Condens. Matter **9**, 2179 (1997).
[31] A. Arya, S. Banerjee, G. P. Das, I. Dasgupta, T. Saha-Dasgupta, and A. Mookerjee, Acta Mater. **49**, 3575 (2001).
[32] D. Paudyal, T. Saha-Dasgupta, and A. Mookerjee, J. Phys.: Condens. Matter **15**, 1029 (2003).
[33] A. Mookerjee, T. Saha-Dasgupta, I. Dasgupta, A. Arya, S. Banerjee, and G. P. Das, Bull. Mater. Sci. **26**, 79 (2003).
[34] D. Paudyal and A. Mookerjee, J. Phys.: Condens. Matter **16**, 5791 (2004).
[35] D. Paudyal, T. Saha-Dasgupta, and A. Mookerjee, J. Phys.: Condens. Matter **16**, 7247 (2004).
[36] D. Paudyal and A. Mookerjee, Physica B **366**, 55 (2005).
[37] A. Chakrabarti and A. Mookerjee, J. Phys.: Condens. Matter **13**, 10149 (2001).
[38] M. Chakraborty, A. Chakrabarti, and A. Mookerjee, J. Magn. Magn. Mater. **313**, 243 (2007).
[39] Aftab Alam, T. Saha-Dasgupta, A. Mookerjee, A. Chakrabarti, and G. P. Das, Phys. Rev. B **75**, 134203 (2007).
[40] T. Takasugi, O. Izumi, and N. Masahashi, Acta Metall. **33**, 1259 (1985).
[41] B. Gleeson, W. Wang, S. Hayashi, and D. J. Sordelet, Mater. Sci. Forum **461-464**, 213 (2004).
[42] J. L. Kamm and W. W. Milligan, Scr. Metall. Mater. **31**, 1461 (1994).
[43] H. Meininger and M. Ellner, J. Alloys Compds. **353**, 207 (2003).
[44] C. Y. Geng, C. Y. Yang, and T. Yu, Acta Mater. B **52**, 5427 (2004).
[45] S. Ochial, Y. Oya, and T. Suzuki, Acta Metall. **32**, 289 (1984).
[46] C. Jiang, D. J. Sordelet, and B. Gleeson, Phys. Rev. B **72**, 184203 (2005).
[47] G. Treglia and F. Ducastelle, J. Phys. F: Met. Phys. **17**, 1935 (1987).
[48] P. P. Singh, A. Gonis, and P. E. A. Turchi, Phys. Rev. Lett. **71**, 1605 (1993).
[49] Z. W. Lu, S. H. Wei, and A. Zunger, Phys. Rev. Lett. **66**, 1753 (1991).
[50] Z. W. Lu, S. H. Wei, and A. Zunger, Phys. Rev. Lett. **68**, 1961 (1992).
[51] N. R. Burke, Surf. Sci. **58**, 349 (1976).
[52] O. Jepsen, O. K. Andersen, and A. R. Mackintosh, Phys. Rev. B **12**, 3084 (1975).
[53] R. Haydock, Solid State Phys. **35**, 216 (1980).
[54] N. Beer and D. G. Pettifor, in *Electronic Structure of Complex Systems*, edited by P. Phariseau and W. M. Tammerman (Plenum, New York, 1984), p. 769.
[55] R. Haydock, V. Heine, and M. J. Kelly, J. Phys. C **5**, 2845 (1972).
[56] P. E. A. Turchi, G. M. Stocks, W. H. Butler, D. M. Nicholson, and A. Gonis, Phys. Rev. B **37**, 5982 (1988).
[57] P. C. Clapp and S. C. Moss, Phys. Rev. **142**, 418 (1966); **171**, 754 (1968).
[58] R. V. Chepulskii and V. N. Bugaev, J. Phys.: Condens. Matter **10**, 7327 (1998).
[59] K. K. Saha, T. Saha-Dasgupta, A. Mookerjee, and I. Dasgupta, J. Phys.: Condens. Matter **16**, 1409 (2004).
[60] J. Kudrnovský and V. Drchal, Phys. Rev. B **41**, 7515 (1990).